

Received Date : 25-Feb-2014

Revised Date : 02-Apr-2014

Accepted Date : 30-Apr-2014

Article type : Research Article

Design, synthesis, and evaluation of 7H-thiazolo[3,2-b]-1,2,4-triazin-7-one derivatives as dual binding site acetylcholinesterase inhibitors

Sijie Liu¹, Ruofeng Shang^{2*}, Lanxiang Shi¹, Ran Zhou¹, Jinyu He¹, David Chi-Cheong Wan³

¹College of Chemical Engineering, Shijiazhuang University, Shijiazhuang 050035, PR China

²Key Laboratory of New Animal Drug Project of Gansu Province; Key Laboratory of Veterinary Pharmaceutical Development, Ministry of Agriculture, P. R. China; Lanzhou Institute of Husbandry and Pharmaceutical Sciences of CAAS, Lanzhou 730050, PR China

³Department of Biochemistry, The Chinese University of Hong Kong, Hong Kong SAR, PR China

*Corresponding author: Tel.: +86 931 2115286; fax: +86 931 2115951. E-mail address:

shangrf1974@163.com

Abstract: New dual binding site acetylcholinesterase (AChE) inhibitors have been designed and synthesized as a new drug candidate for the treatment of Alzheimer's disease (AD) through the binding to both catalytic and peripheral sites of the enzyme. Therefore, a series of 7H-thiazolo[3,2-b]-1,2,4-triazin-7-one derivatives

This article has been accepted for publication and undergone full peer review but has not been through the copyediting, typesetting, pagination and proofreading process which may lead to differences between this version and the Version of Record. Please cite this article as an 'Accepted Article', doi: 10.1111/cbdd.12362

This article is protected by copyright. All rights reserved.

6a-j were synthesized and investigated for their ability to inhibit the activity of human AChE (*hAChE*) in comparison with huperzine-A. All the compounds were found to inhibit AChE activity, especially compounds **6c** and **6i** with the inhibition value of 76.10 and 77.82%, respectively. The molecular docking study indicated that they were nicely accommodated by AChE. The molecular docking study revealed that **6c** and **6i** possessed a more optimal binding conformation than **6a** and can perfectly fit into the active and peripheral site of *hAChE*, and consequently exhibited highly improved inhibitor potency to *hAChE*.

Keywords: acetylcholinesterase; synthesis; inhibitors; 7*H*-thiazolo[3,2-*b*]-1,2,4-triazin-7-one derivatives; docking; Alzheimer's disease

Introduction

Alzheimer's disease (AD) is described by Dr. Alois Alzheimer in 1907 as a neurodegenerative disorder. It affects over 20 million individuals worldwide and this number will substantially increase in the future along with the increase of the number of elderly in the population [1]. AD leads to a progressive decline of the cognitive function, executive function losses, memory deficits, and eventually to incapacitating dementia before death [2, 3]. The proven and currently accepted therapeutic approach for the treatment of AD involves the inhibition of the enzyme acetylcholinesterase (AChE) which is responsible for the hydrolysis of acetylcholine (ACh), thereby raising the levels of ACh in the synaptic cleft [4]. Five cholinesterase inhibitors tacrine, donepezil, rivastigmine, huperzine-A and galantamine (Figure 1) are approved by the US Food and Drug Administration (FDA) and are currently in the market [5].

X-ray structures of AChE co-crystallized with various ligands provided insights into the essential structural elements and motifs central to its catalytic mechanism and mode of ACh processing. One of the striking structural features of the *Torpedo californica* AChE (*TcAChE*) from the X-ray analysis is the presence of a narrow, long, hydrophobic gorge which is approximately 20 Å deep [6]. The catalytic active site (CAS) is the binding site of classical AChE inhibitors, such as tacrine and huperzine A, which has been studied thoroughly. The CAS comprising Ser203, Glu334 and His447 interacts with the cationic substrates, for example ACh. The esteratic locus of the aromatic gorge also interacts with hydrophobic substrates and ligands. Interactions between quaternary ammonium functionality of many ligands and the side chains of Trp86, Glu202, and Tyr337, and the phenolic oxygen of Tyr133 are found in the anionic binding site near the CAS [7]. Additionally, there is a peripheral anionic site (PAS) composed of Tyr72, Asp74, Tyr124 and Trp286 which located at the gorge entrance. But the function of the PAS has not been elucidated clearly as yet. Recent studies have demonstrated that the PAS might accelerate the aggregation and deposition of β -amyloid peptide which are considered as another cause of AD [8]. Therefore, the ideal AChE inhibitors should bind to the CAS and PAS simultaneously and disrupt the interactions between the enzyme and the β -amyloid peptide, and then slow down the progression of the disease.

This article is protected by copyright. All rights reserved.

In an earlier report, we have presented the preparation and evaluation of some new 7H-thiazolo[3,2-b]-1,2,4-triazin-7-one derivatives as AChE inhibitors which interacted with the PAS and the CAS of AChE [9-11]. Most of these compounds proved to be potent AChE inhibitors in vitro, among which compounds bearing two substituents on the aryl ring at C3 position of parent nucleus ring showed the most activity. Following these reasons and in pursuit of our previous study a series of new 7H-thiazolo[3,2-b]-1,2,4-triazin-7-one derivatives were designed, synthesized and evaluated for AChE inhibitory activities. The final compounds have been tested for their ability to inhibit AChE using Ellman's method [12].

Materials and Methods

Chemistry

Reagents and solvents were purchased from common commercial suppliers and were used without further purification. All melting points were taken in open capillary tubes and are uncorrected. Nuclear magnetic resonance spectra were recorded in CDCl₃ or DMSO solutions, using Bruker 300 MHz spectrometers or 600 MHz spectrometers. The mass spectra (MS) were obtained by electronic impact (EI) at 70eV in an Agilent spectrometer (with direct insertion probe) or by electrospray (ESI) in a Waters spectrometer. The IR spectra were obtained using a Perkin-Elmer 298 spectrometer (Perkin-Elmer, Norwalk, CT, USA).

4-[(4-Methoxyphenyl)methylene]-2-methyl-5(4H)-oxazolone (**1**),
2-Acetamido-3-(4-methoxyphenyl)-2-propenoic acid (**2**), 4-Methoxyphenylpyruvic acid (**3**),
6-(4-Methoxybenzyl)-3,4-dihydro-3-thioxo-1,2,4-triazin-5(2H)-one (**4**) and
6-(4-methoxybenzyl)-3-hydroxyphenyl-7H-thiazolo[3,2-b]-1,2,4-triazin-7-ones (**5**) were prepared by previously reported procedures[9].

General procedure for synthesis of 6-(4-methoxybenzyl)-3-aryl-7H-thiazolo[3,2-b]-1,2,4-triazin-7-ones (**6**)

6-(4-methoxybenzyl)-3-hydroxyphenyl-7H-thiazolo[3,2-b]-1,2,4-triazin-7-one (**5a-b**) (10 mmol) was solved in acetone (20mL), K₂CO₃ (2g) and alkyl chloride (10 mmol) were added, and refluxed for 8-24h until the TLC assay indicated that the reaction was completed. The mixture was filtered, and evaporated to remove solvents. The residues were collected and recrystallized from ethanol, to give the target compounds **6a-j**.

6-(4-methoxybenzyl)-3-{4-[2-(dimethylamino)ethoxy]phenyl}-7H-thiazolo[3,2-b]-1,2,4-triazin-7-one (6a**):** white crystal, 41.2% yield; mp: 176-178°C; ¹H-NMR (300 MHz, CDCl₃): δ 7.47 (2H, d, *J* = 8.7Hz), 7.27 (2H, d, *J* = 9.0Hz), 6.97 (2H, d, *J* = 9.0Hz), 6.83 (2H, d, *J* = 8.7Hz), 6.71 (1H, s), 4.14 (2H, t), 4.05 (2H, s), 3.79 (3H, s), 2.80 (2H, t), 2.39 (6H, s); ESI-MS (*m/z*): 437.0 (M+H)⁺; IR (KBr): ν 2930, 1624, 1477, 1384, 1251, 1178, 1034, 810 cm⁻¹.

6-(4-methoxybenzyl)-3-{4-[2-(1-piperidinyl)ethoxy]phenyl}-7H-thiazolo[3,2-b]-1,2,4-triazin-7-one (6b**):** yellow crystal, 36.7% yield; mp: 171-173°C; ¹H-NMR (300 MHz, CDCl₃): δ 7.47 (2H, d, *J* = 8.7Hz), 7.27 (2H, d, *J* =

This article is protected by copyright. All rights reserved.

8.4Hz), 6.94 (2H, d, $J = 8.7\text{Hz}$), 6.83 (2H, d, $J = 8.4\text{Hz}$), 6.72 (1H, s), 4.20 (2H, t), 4.05 (2H, s), 3.79 (3H, s), 2.86 (2H, t), 2.59 (4H, s), 1.64 (4H, s), 1.49 (2H, s); ESI-MS (m/z): 477.7 ($M+H$)⁺; IR (KBr): ν 3020, 2933, 1632, 1580, 1512, 1479, 1385, 1355, 1300, 1252, 1180, 1118, 1035, 760 cm^{-1} .

6-(4-methoxybenzyl)-3-{3-methyl-4-[2-(dimethylamino)ethoxy]phenyl}-7H-thiazolo[3,2-b]-1,2,4-triazin-7-one (6c): yellow crystal, 32.2% yield; mp: 157-158 $^{\circ}$; ¹H-NMR (600 MHz, CDCl₃): δ 7.35 (1H, d), 7.32 (1H, s), 7.28 (2H, d, $J = 8.4\text{Hz}$), 6.84 (1H, d), 6.83 (2H, d, $J = 8.4\text{Hz}$), 6.68 (1H, s), 4.17 (2H, t), 4.05 (2H, s), 3.78 (3H, s), 2.84 (2H, t), 2.40 (6H, s), 2.25 (3H, s); ESI-MS (m/z): 451.0 ($M+H$)⁺; IR (KBr): ν 2939, 1630, 1487, 1384, 1301, 1247, 1177, 1135, 1034, 800 cm^{-1} .

6-(4-methoxybenzyl)-3-{3-methyl-4-[2-(1-piperidinyl)ethoxy]phenyl}-7H-thiazolo[3,2-b]-1,2,4-triazin-7-one (6d): yellow crystal, 45.9% yield; mp: 165-166 $^{\circ}$; ¹H-NMR (600 MHz, CDCl₃): δ 7.36 (1H, d), 7.32 (1H, s), 7.29 (2H, d, $J = 8.4\text{Hz}$), 6.84 (1H, d), 6.83 (2H, d, $J = 8.4\text{Hz}$), 6.68 (1H, s), 4.21 (2H, s), 4.06 (2H, s), 3.80 (3H, s), 2.90 (2H, s), 2.59 (4H, s), 2.24 (3H, s), 1.65 (4H, s), 1.48 (2H, s); ESI-MS (m/z): 491.0 ($M+H$)⁺, 981.0 ($2M+H$)⁺; IR (KBr): ν 3067, 2933, 2852, 1632, 1565, 1513, 1486, 1384, 1356, 1302, 1248, 1177, 1135, 1034, 952, 863, 802, 764 cm^{-1} .

6-(4-methoxybenzyl)-3-{3-methyl-4-[2-(4-morpholinyl)ethoxy]phenyl}-7H-thiazolo[3,2-b]-1,2,4-triazin-7-one (6e): yellow crystal, 41.6% yield; mp: 162-164 $^{\circ}$; ¹H-NMR (300 MHz, CDCl₃): δ 7.28~7.35 (4H, m), 6.85 (3H, m), 6.70 (1H, s), 4.21 (2H, t), 4.07 (2H, s), 3.80 (3H, s), 3.77 (4H, m), 2.90 (2H, t), 2.66 (4H, m), 2.26 (3H, s); ESI-MS (m/z): 493.0 ($M+H$)⁺, 985.9 ($2M+H$)⁺; IR (KBr): ν 2932, 1636, 1489, 1384, 1248, 1118 cm^{-1} .

6-(4-methoxybenzyl)-3-{3-methyl-4-[2-(diethylamino)ethoxy]phenyl}-7H-thiazolo[3,2-b]-1,2,4-triazin-7-one (6f): yellow crystal, 35.5% yield; mp: 158-159 $^{\circ}$; ¹H-NMR (300 MHz, CDCl₃): δ 7.29~7.37 (4H, m), 6.84 (3H, t), 6.67 (1H, s), 4.12 (2H, t), 4.05 (2H, s), 3.78 (3H, s), 2.96 (2H, t), 2.69 (4H, m), 2.24 (3H, s), 1.11 (6H, m); ESI-MS (m/z): 479.1 ($M+H$)⁺; IR (KBr): ν 2967, 1628, 1487, 1384, 1302, 1259, 1176, 1136, 1038, 800 cm^{-1} .

6-(4-methoxybenzyl)-3-{3-methyl-4-[2-(1-piperidinyl)-2-oxoethoxy]phenyl}-7H-thiazolo[3,2-b]-1,2,4-triazin-7-one (6g): yellow crystal, 32.7% yield; mp: 133-134 $^{\circ}$; ¹H-NMR (300 MHz, CDCl₃): δ 7.36 (1H, d), 7.32 (1H, s), 7.29 (2H, d, $J = 8.4\text{Hz}$), 6.84 (1H, d), 6.83 (2H, d, $J = 8.4\text{Hz}$), 6.68 (1H, s), 4.76 (2H, s), 4.05 (2H, s), 3.79 (3H, s), 3.59 (2H, s), 2.54 (2H, s), 2.29 (3H, s), 1.65 (4H, s), 1.48 (2H, s); ESI-MS (m/z): 505.0 ($M+H$)⁺; IR (KBr): ν 2935, 2856, 1637, 1513, 1481, 1384, 1302, 1248, 1177, 1135, 1032, 807, 758 cm^{-1} .

6-(4-methoxybenzyl)-3-{3-methyl-4-[2-(4-morpholinyl)-2-oxoethoxy]phenyl}-7H-thiazolo[3,2-b]-1,2,4-triazin-7-one (6h): yellow crystal, 33.6% yield; mp: 152-154 $^{\circ}$; ¹H-NMR (300 MHz, CDCl₃): δ 7.37 (2H, d), 7.29 (2H, d, $J = 8.5\text{Hz}$), 6.90 (1H, d), 6.84 (2H, d, $J = 8.5\text{Hz}$), 6.71 (1H, s), 4.81 (2H, s), 4.10 (2H, s), 3.80 (3H, s), 3.68 (8H, m), 2.29 (3H, s); ESI-MS (m/z): 507.0 ($M+H$)⁺; IR (KBr): ν 3096, 2963, 2853, 1632, 1570, 1513, 1482, 1384, 1359, 1302, 1248, 1177, 1135, 1116, 1068, 1031, 971, 819, 750 cm^{-1} .

6-(4-methoxybenzyl)-3-{3-methyl-4-[(2-diethylamino)-2-oxoethoxy]phenyl}-7H-thiazolo[3,2-b]-1,2,4-triazin-7-one (6i): yellow crystal, 37.6% yield; mp: 132-134 $^{\circ}$; ¹H-NMR (300 MHz, CDCl₃): δ 7.37 (2H, d), 7.29 (2H, d), 6.86 (3H, t), 6.70 (1H, s), 4.80 (2H, s), 4.06 (2H, s), 3.80 (3H, s), 3.46 (4H, m), 2.31 (3H, s), 1.27 (3H, t), 1.19

(3H, t); ESI-MS (m/z): 493.0 (M+H)⁺; IR (KBr): ν 3067, 2933, 1634, 1567, 1513, 1481, 1383, 160, 1302, 1249, 1177, 1134, 1070, 1033, 867, 800, 757 cm⁻¹.

6-(4-methoxybenzyl)-3-{3-methyl-4-[2-(dimethylamino)-2-oxoethoxy]phenyl}-7H-thiazolo[3,2-b]-1,2,4-triazin-7-one (6j): yellow crystal, 34.4% yield; mp: 126-127°C; ¹H-NMR (300 MHz, CDCl₃): δ 7.26~7.34 (4H, t), 6.85 (3H, d), 6.70 (1H, s), 4.80 (2H, s), 4.05 (2H, s), 3.80 (3H, s), 3.14 (3H, s), 3.02 (3H, s), 2.37 (3H, s); ESI-MS (m/z): 465.0 (M+H)⁺; IR (KBr): ν 3076, 2928, 1637, 1565, 1513, 1485, 1402, 1384, 1353, 1302, 1247, 1177, 1134, 1034, 800, 762 cm⁻¹.

Inhibition of AChE

The inhibitory potency against AChE was evaluated by means of Ellman's test [13]. AChE stock solution was prepared by dissolving *h*AChE 0.5 unit in 100 mM PBS buffer (pH 7.4). The synthesized compounds **6a-j** (10 μ M) were dissolved in DMSO. The assay solution consisted of 100 mM PBS buffer (pH 7.4), with the addition of 10 mM 5'-dithio-bis-(2-nitrobenzoate) (DTNB, Sigma, D-8130), AChE (5 μ L), drug (10 μ L), and 12.5 mM acetylthiocholine iodide (ATCh) water solution. The final assay volume was 900 μ L. After incubation at 37°C for about 15 min, the mixture was added 50 μ L ATCh and 50 μ L DTNB, followed by incubation at 37°C for 20 min with continuous gentle shake until the color change to yellow. Inhibitory effects were expressed as the percentage of inhibition.

Docking studies

To disclose a possible binding mode of compounds **6a-j** with *h*AChE enzyme's binding pockets, the docking simulation were performed using the available crystallographic structure of enzyme (PDB ID: 4EY7) [14] using AutoDock 4.0. In order to obtain the better results from docking protocols, water molecules and other ligand (NAG) were excluded. The polar hydrogen atoms of the enzyme were added, the non-polar hydrogen atoms were merged and Gasteiger charges were assigned. For all ligands the non-polar hydrogen atoms were merged, and the Gasteiger charges were assigned. The grid box dimensions were 60 \times 60 \times 60 Å around the active site and the grid spacing was set to 0.375 Å. Docking was performed using the empirical free energy function together with the Lamarckian genetic algorithm (LGA). The LGA protocol applied a population size of 150 individuals, while 250,000 energy evaluations were used for the 20 LGA runs. In addition, the maximum number of evaluations was set to 27,000. In this study, the co-crystal natural substrate, donepezil, was taken out of the active site and docked again used as the template for molecular alignment. The cluster analyses were computed with a cluster tolerance by less than 1.5 Å in positional root-mean-square deviation. PyMol 1.5.0.3 software was used for visualization of protein-ligand interactions.

Results and Discussion

Chemistry

The target compounds **6a-j** were synthesized as illustrated in Scheme 1. At the first stage, anisaldehyde was cyclized with N-acetylglycine in acetic anhydride, which led to a high yield of 4-(arylmethylene)-2-methyl-5(4*H*)-oxazolone **1**. **1** converted to intermediate 2-Acetamido-3-(4-methoxyphenyl)-2-propenoic acid **2** with acetone and water. Intermediate **2** was further hydrolyzed with 1 N hydrochloric acid to give 4-methoxyphenylpyruvic acid **3**. The base-catalysed condensation reaction of 4-methoxyphenylpyruvic acid **3** with thiosemicarbazone in the presence of ethyl alcohol and 50 % NaOH, followed by neutralisation in the presence of cold HCl that yielded 6-(4-methoxybenzyl)-3,4-dihydro-3-thioxo-1,2,4-triazin-5(2*H*)-one **4**. Subsequently, the differently substituted phenacyl chloride and **4** underwent intra-molecular cyclization on refluxing with glacial acetic acid to yield 6-(4-methoxybenzyl)-3-hydroxyphenyl-7*H*-thiazolo[3,2-*b*]-1,2,4-triazin-7-ones **5a-b**. There after refluxing of the compounds (5a-b) with different substituted alkyl chloride in the presence of acetone and K₂CO₃ provided 6-(4-methoxybenzyl)-3-aryl-7*H*-thiazolo [3,2-*b*]-1,2,4-triazin-7-ones **6a-j**.

Inhibition of AChE

As shown in Table 1, 6-(4-methoxybenzyl)-3-aryl-7*H*-thiazolo [3,2-*b*]-1,2,4-triazin-7-one derivatives **6a-j** generally showed moderate to good *hAChE* inhibitory activities with inhibition values ranging from 37.80% to 77.82%. Among all the derivatives examined, compound **6i** showed the most inhibitory activity and the inhibition reached to 77.82%. However, all the synthesized compounds showed lower inhibitory activity than the reference drug huperzine-A.

It was observed that the type and position of the substituents played an important role for the inhibitory activities. As compared with the single substituent on the *para*-position of the phenyl group derivative **6a** and **6b** (37.80% and 54.67%), the two substituents on the *meta* and *para*-position of the phenyl group derivatives **6c** and **6d** showed increased activity (76.10% and 73.92%). On the other hand, the replacement of the piperidinyl group of compound **6d** and **6g** by morpholinyl group (compound **6e** and **6h**) resulted in the decreased activity.

Docking studies

To investigate the binding mode of the series of 7*H*-thiazolo[3,2-*b*]-1,2,4-triazin-7-one derivatives, docking simulations were performed with Autodock 4 software. The model of the receptor was based on the crystal structure of *hAChE* complex with donepezil (PDB ID: 4EY7). The co-crystal natural substrate was taken out of the active site and docked again. The top 3 docking configurations were taken into consideration to validate

the results and the RMSD was calculated for each configuration in comparison with the co-crystallized ligand, donepezil. The acceptable results (RMSD within 0.61-0.83Å) indicated that the docked configurations have similar binding positions and orientations within the binding site and are similar to the co-crystal structure, which illustrates the fact that the docking protocols used could successfully generate the crystal donepezil-AChE complex precisely. The pose (best conformation of docked donepezil) selection of docked ligands was done based on the closest alignment to the original donepezil ligand as well as the interaction of ligands with key amino acid residues such as Ser203, His447 at the CAS and Tyr72, Asp74, Trp286 at PAS. The benzyl ring stacks against Trp86 near the active site, while the indanone ring stacks against Trp286 in the peripheral anionic site. The docking simulations reveal all target compounds exhibited multiple binding modes with the human AChE (Figure 2). The calculations with the flexible docking protocol placed all the compounds correctly into the binding pocket as presented in Figure 3. The docking results revealed the three compounds could suitably interact with the CAS and PAS of the enzyme. For example, the docking simulation revealed that 4EY7 and compounds **6a**, **6c** and **6i** interacted through π - π aromatic interactions and hydrogen bonding (Figure 4). Both the phenyl ring of the compounds **6a**, **6c** and **6i** may show π - π interactions with Trp86. The nitrogen atom of side chain may also show cation- π interactions with Tyr341 (one of the six residues of PAS clustered around the entrance to the active site gorge) with the distance of 4.6, 3.6 and 3.9 Å, respectively. Additional significant H-bond interactions were also observed between the oxygen atom of **6c** with -OH group of Tyr133, Tyr124 and Tyr337 with the distance of 2.8 Å, 3.0 Å and 2.5 Å respectively. Tyr133 and Tyr337 are important residues of "Anionic binding site" in the gorge which involved in optimally positioning the ester at the acylation site along with binding to trimethylammonium choline through cation- π interactions. For the compound **6i**, more H-bond interactions with Tyr124, Trp86 and Tyr449 were found, which might be the reason for its increased inhibitory potency.

Conclusion

Starting with anisaldehyde, a new series of 7H-thiazolo[3,2-b]-1,2,4-triazin-7-one derivatives were designed and synthesized as dual binding site inhibitors of AChE. All these new derivatives have been investigated for their inhibitory activity *in vitro* using Ellman's method. The results revealed that most compounds with moderate inhibitory activity. Among them, compounds **6i** bearing diethylamino-2-oxoethoxy in the aryl ring at C4 position exerts the most potency. Molecular docking results revealed that **6a**, **6c** and **6i** might behave as dual binding site inhibitors. Compound **6c** with two substituents on the *meta* and *para* position of the phenyl group show the better binding conformation than **6a**. These studies suggest that 7H-thiazolo[3,2-b]-1,2,4-triazin-7-one derivatives with two substituents may be a promising structural template for the development of novel AChE inhibitors in managing amnesic disorders including AD.

Conflict of Interest

The author(s) confirm that this article content has no conflicts of interest.

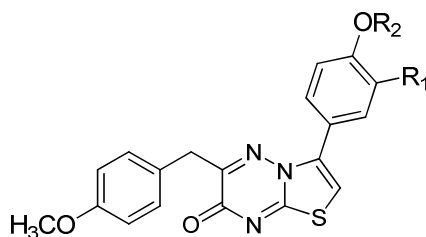
This article is protected by copyright. All rights reserved.

References

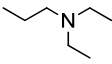
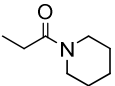
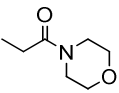
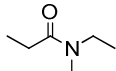
- [1] Anand P., Singh B. (2013) Synthesis and evaluation of novel carbamate-substituted flavanone derivatives as potent acetylcholinesterase inhibitors and anti-amnestic agents. *Med Chem Res*;22:1648-1659.
- [2] Ahmad M. F., Aram A., Hamid N., Alireza A. (2013) Synthesis, docking and acetylcholinesterase inhibitory assessment of 2-(2-(4-Benzylpiperazin-1-yl)ethyl)isoindoline-1,3-dione derivatives with potential anti-Alzheimer effects. *DARU J Pharm Sci*;21:47-56.
- [3] Meng F.C., Mao F., Shan W. J., Qin F.F., Huang L., Li X.S. (2012) Design, synthesis, and evaluation of indanone derivatives as acetylcholinesterase inhibitors and metal-chelating agents. *Bioorg Med Chem*;22:4462-4466.
- [4] Pepeu G., Giovannini M.G. (2009) Cholinesterase inhibitors and beyond. *Curr Alzheimer Res*;6:86-96.
- [5] Ucar G., Gokhan N.A., Yesilada A.B. (2005) 1-N-Substituted thiocarbamoyl-3-phenyl-5-thienyl-2-pyrazolines: a novel cholinesterase and selective monoamine oxidase B inhibitors for the treatment of Parkinson's and Alzheimer's diseases. *Neurosci Lett*;382:327-331.
- [6] Lu S.H., Wu J.W., Liu H.L., Zhao J. H., Liu K.T. (2011) The discovery of potential acetylcholinesterase inhibitors: a combination of pharmacophore modeling, virtual screening, and molecular docking studies. *J Biomed Sci*;18:8-13.
- [7] Khalid A., Zaheer H., Anjum S.M., Khan R., Atta R. (2004) Kinetics and structure-activity relationship studies on pregnane-type steroidal alkaloids that inhibit cholinesterases. *Bioorg Med Chem*;12:1995-2003.
- [8] Chitranshi N., Gupta S., Tripathi P.K., Seth P.K. (2013) New molecular scaffolds for the design of Alzheimer's acetylcholinesterase inhibitors identified using ligand and receptor-based virtual screening. *Med Chem Res*;22:2328-2345.
- [9] Liu S.J., Yang L., Jin Z., Huang E., Wan D., Lin H., Hu C. (2009) Design, synthesis, and biological evaluation of 7H-thiazolo[3,2-b]-1,2,4-triazin-7-one derivatives as novel acetylcholinesterase inhibitors. *ARKIVOC*;10:333-348.
- [10] Liu, S. J.; Yang, L.; Liu, X.; Wan, D.; Lin, H.; Hu, C. (2010) Design, Synthesis, and Biological Evaluation of 7H-thiazolo[3,2-b]-1,2,4-triazin-7-one Derivatives as Acetylcholinesterase Inhibitors. *Lett Drug Des Discov*;7:5-8.

- [11] Xu H.; Jin Z., Liu S., Liu H., Wan D., Hu C. (2012) Design, synthesis characterization and in vitro biological activity of a series of 3-aryl-6-(bromoarylmethyl)-7H thiazolo[3,2-b]-1,2,4-triazin-7-one derivatives as the novel acetylcholinesterase inhibitors. *Chin Chem Lett*;23:65-772.
- [12] Elsinghorst P.W., Tanarro C.M., Gütschow M. (2006) Novel heterobivalent tacrine derivatives as cholinesterase inhibitors with notable selectivity toward butyrylcholinesterase. *J Med Chem*; 49: 7540-7544.
- [13] Ellman G.L., Courtney K.D., Andres V.J., Featherstone R.M.A. (1961) A new and rapid colorimetric determination of acetylcholinesterase activity. *Biochem Pharmacol*;7:88-90.
- [14] Kryger G., Harel M., Giles K., Toker L., Velan B., Lazar A., Kronman C., Barak D., Ariel N., Shafferman A., Silman I., Sussman J.L. (2000) Structures of recombinant native and E202Q mutant human acetylcholinesterase complexed with the snake-venom toxin fasciculin-II. *Acta Crystallogr Sect D*;56:1385-1394.

Table 1. Inhibition of *hAChE* Activities by the targets at 10 μ M (n=2)



No.	R ₁	R ₂	Inhibition (%)
6a	H		37.80
6b	H		54.67
6c	CH ₃		76.10
6d	CH ₃		73.92
6e	CH ₃		56.26

6f	CH ₃		66.14
6g	CH ₃		70.48
6h	CH ₃		43.06
6i	CH ₃		77.82
6j	CH ₃		71.82
huperzine-A			100.00

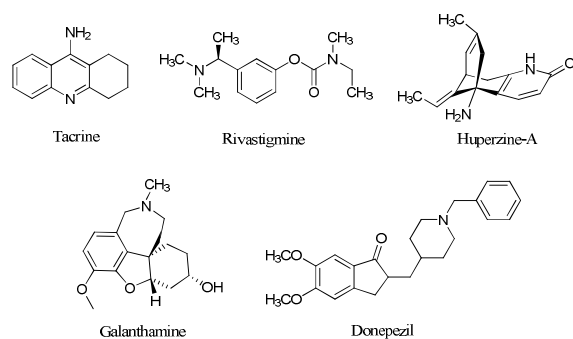


Figure 1. Structure of reported AChE inhibitors.

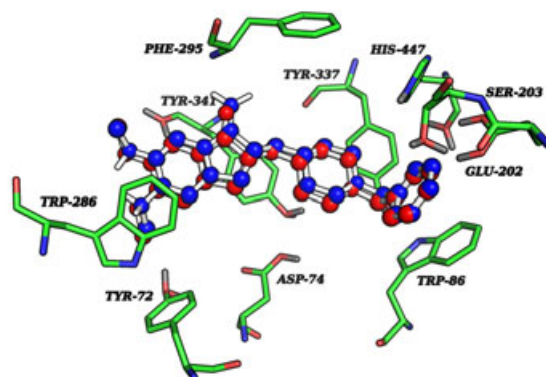


Figure 2. Binding orientation of redocked co-crystal donepezil (blue) and original donepezil (red).

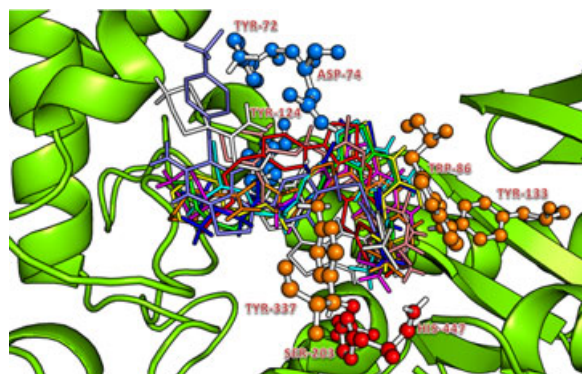


Figure 3. Superimposition of docking conformations of **6a** (red), **6b** (green), **6c** (blue), **6d** (yellow), **6e** (magenta), **6f** (cyan), **6g** (orange), **6h** (white), **6i** (salmon) and **6j** (slate) inside the gorge of 4EY7 which were showed as sticks. Only a part of residues of PAS (red), CAS (blue) and anionic binding site (yellow) of 4EY7 were showed as ball and stick to reveal the binding gorge. Some residues of protein were omitted for clarity.

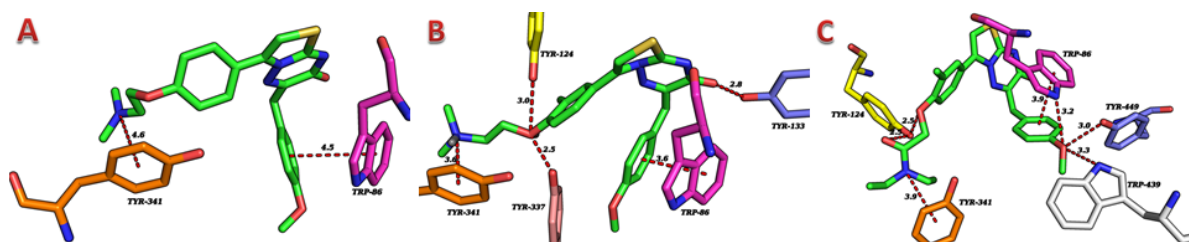
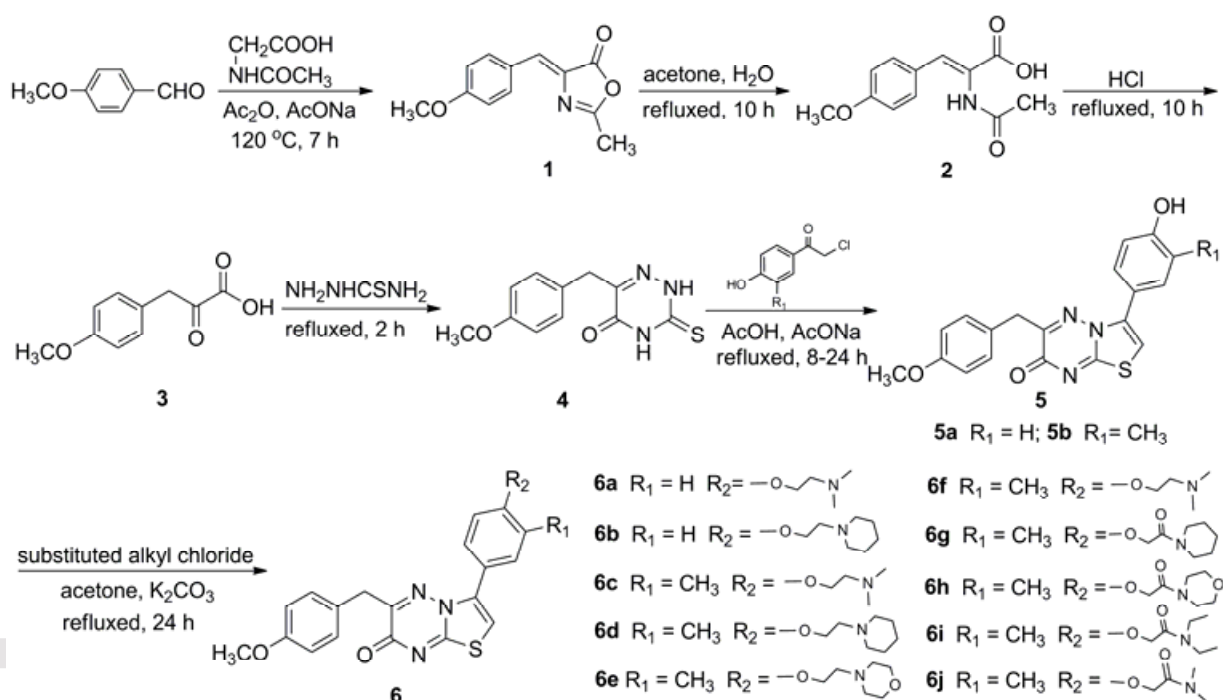


Figure 4. Docking of compounds **6a** (A), **6c** (B) and **6i** (C) to 4EY7. The compounds **6a**, **6c** and **6i** are colored by green. The hydrogen bonds, π - π and cation- π interactions are shown as red dashed lines.



Scheme 1. The synthetic route of 7H-thiazolo[3,2-b]-1,2,4-triazin-7-one derivatives